Understanding the R_0 of Epidemics

Harisankar Ramaswamy[1], Assad A. Oberai[1], Mitul Luhar[1] and Yannis C. Yortsos[1]

[1]*University of Southern California*
Los Angeles, CA 90089, USA
hramaswa@usc.edu, aoberai@usc.edu, luhar@usc.edu, yortsos@usc.edu

Abstract. A fundamental parameter in the epidemiology of infections is the so-called basic reproduction number, R_0, loosely defined as the number of new infections an infected individual will subsequently cause. This parameter is central to traditional SIR models and plays a key role in dictating transmission dynamics. However, R_0 is typically ill-defined since it does not specify the time interval over which such secondary infections will occur. In SIR models, R_0 also has a different interpretation depending on the assumed kinetics of infection. In this paper, we borrow concepts from a recent publication [1] to provide explicit expressions for R_0 in terms of key physio-chemical, environmental, and operational parameters, including the spatial population density, which is fundamental to the health policy of spatial distancing. We then explore how R_0 varies depending on the kinetics assumed, motivated by the special case of interactions in enclosed environments for which the SIR model needs to be reformulated. We consider, as a special case, super-spreader events, where we show that if one were to use the SIR model, the effective value of R_0 will be a significantly large, albeit decreasing, function of the duration of the event, suggesting a delta-function-like behavior. We comment on a possible extension of the SIR model to capture different infection kinetics by introducing an additional dimensionless number m, which represents the one-to-m collision mechanism expected for the spread of infections in enclosed or high-density environments.

Keywords: Epidemics, Reproduction Number, SIR Model

1 Introduction

The spread of epidemics, such as COVID-19, has been traditionally addressed using a number of models in which the so-called basic reproduction number R_0, roughly defined as the number of new infections an infected individual will subsequently cause, plays an important role. This parameter is central to traditional SIR models [2, 3] and plays a key role in dictating transmission dynamics. However, its relation to fundamental parameters, such as spatial density, the kinetics of transmission of infection, and the mobility of populations (via dispersion or advection) and other parameters, is not well understood. In a recent paper [1], we provided a comprehensive model for the propagation of infection, based on an analogy with chemical reaction models, that provides a solid foundation for the spreading of epidemics and delineates the dependence of R_0 on measurable parameters. In that model we proceeded with the standard SIR assumption [2, 3] that infection is the result of one-to-one interaction between two individual species (susceptible and infected), where infection occurs at a certain rate following such encounters. Specifically, we modeled the process with an equivalent chemical reaction scheme

$$S + I \quad \mapsto \quad 2I \tag{1}$$

$$I \quad \mapsto \quad R \tag{2}$$

where S denotes susceptible, I denotes infected and R denotes recovered (or perished) populations. An interesting question is to inquire whether or not such a scheme also applies to different modes of infection; for example, those occurring in enclosed environments, which enable the possibility that an infected individual can simultaneously infect multiple susceptible ones. For diseases such as COVID-19, which are transmitted via droplets and aerosols, indoor gatherings, characterized by a number of people in close proximity (i.e., high spatial density) actively vocalizing or interacting with one another [see e.g., 4, 5], will likely have different dynamics than the one-to-one SIR-like model described in (1)-(2). A particularly relevant application involves so-called super-spreader

events, which have been known to play a critical role in the spreading dynamics of infectious diseases. Including super-spreader events in conventional SIR models is particularly challenging given the vastly different time scales associated with infection progression ($O(10)$ days for COVID-19) and event duration (typically $O(1)$ hour).

In this paper, we reconcile the dynamics modeled in conventional SIR models with those expected in enclosed environments for events of short duration. Our results suggest new extensions to the conventional SIR dynamics in order to capture different modes of interaction and their kinetics. The remainder of this paper is organized as follows. We first describe the fundamentals of the SIR model and explore how to connect it with enclosed environments events that obey different infection kinetics involving infected *individuals* who are responsible for spreading the disease to a large number of susceptible individuals [6, 7]. We identify the corresponding R_0 number and comment on its value for COVID-19 super-spreader events [1]. We also comment on an extension of the SIR model to capture different kinetics by introducing an additional dimensionless number $m(\geq 1)$, which represents the one-to-m collision mechanism for the spread of infections in enclosed or other high-density environments.

2 Model Formulation and Predictions

We first summarize the key results obtained in [1] where a continuum model was formulated in terms of the population spatial density ρ (number of people/area) and the relative population (species) fractions, $s = \rho_s/\rho$, $i = \rho_i/\rho$, and $r = \rho_r/\rho$ and their variation in time and space, and where ρ_n denotes the spatial density of species n. The corresponding species conservation equations, expressed in dimensionless notation, read as follows, :

$$\frac{\partial s}{\partial t} + Da\nabla\cdot(\mathbf{v}s) - C\nabla(\ln\rho)\cdot\nabla s = \nabla\cdot(C\nabla s) - R_0(\rho,r)si \tag{3}$$

$$\frac{\partial i}{\partial t} + Da\nabla\cdot(\mathbf{v}i) - C\nabla(\ln\rho)\cdot\nabla i = \nabla\cdot(C\nabla s) + R_0(\rho,r)si - i \tag{4}$$

$$\frac{\partial r}{\partial t} + Da\nabla\cdot(\mathbf{v}r) - C\nabla(\ln\rho)\cdot\nabla r = \nabla\cdot(C\nabla r) + i \tag{5}$$

$$\frac{\partial \rho}{\partial t} + Da\nabla\cdot(\mathbf{v}\rho) = 0 \tag{6}$$

where $s + i + r = 1$. In the above, space is normalized by a characteristic length L and time by the characteristic time, T_r, associated with the kinetics of the recovery (assumed to equal 14 days for COVID-19) and we have defined a dimensionless Damkohler number, $Da = UT_r/L$, a dimensionless diffusion number, $C = DT_r/L^2$, and the rescaled velocity $\mathbf{v}$, based on a characteristic dimensional velocity U. We stress that (3)-(6) are expressed in terms of spatial densities, which are the physically relevant variables, rather than in terms of the number of individuals, which is typical in the more traditional SIR-type modeling framework.

Equations (3)-(6) include spatial transport by advection (through Da) and diffusion (through C), and time variation through reaction (conversion of one species to another). Following the key premise of SIR models, we modeled infection and recovery rates in terms of two equivalent irreversible chemical reactions between the species described in (1) and (2). Note that in the RHS of (1) the stoichiometric coefficient 2 implies that a new member of the infected species I is produced as a result of an interaction between a member of I and a member of the susceptible species S. Equation (2) states that a member of species I is converted to the recovered (or perished) species R, which is a statement largely independent of the average rate of the process of infection. The infection rate intensity is characterized by the important dimensionless parameter $R_0(\rho, r)$ which corresponds to the conventional reproduction number and in [1] is explicitly defined as

$$R_0(\rho, r) = \frac{K_0\rho}{\Lambda}\kappa(\rho, r). \tag{7}$$

Equation (7) states that $R_0(\rho, r)$ is proportional to the density ρ, and the kinetic parameter K_0 (dimensions of [time$\times$(number/area)]$^{-1}$) and the dimensionless parameter $\kappa(\rho, r) > 0$. K_0 and $\kappa(\rho, r)$ depend on a number of factors (from spatial distancing to face covering to physiological and environmental parameters). Parameter K_0 implicitly accounts for the frequency of encounters (collisions) between individuals and the intensity of interaction, in addition to biological (infection) and environmental (e.g., face covering) factors. It can capture biological effects such as the increased contagiousness associated with different variants (e.g., as in the current case with the delta variant). Dimensionless parameter $\kappa(\rho, r)$ varies with spatial distancing and the extent of the epidemic, r. For example, beyond a critical distance (below a critical density value ρ_0) we expect that infection rates are negligible ($\kappa(\rho, r) \ll 1$); conversely, there is a maximum limit ρ_1 denoting closest packing where $\kappa(\rho, r)$ takes the value of one. These considerations, as well as the fact that the effect of spatial density in $\kappa(\rho, r)$ should also account for the fraction of recovered individuals r, are further discussed in [1].

In [1] we examined a number of phenomena, including diffusion and advection. However, in this paper we will only consider the *batch reactor* limit, where all spatial gradients in (3)-(6) vanish. The same limit will be considered as we discuss expressions for other kinetic rates, including those for super-spreader events. In a *batch reactor* environment, the resulting equations are similar to the SIR-like model [2, 3, 8]:

$$\dot{s}(t) = -R_0(\rho, r)si \tag{8}$$
$$\dot{i}(t) = R_0(\rho, r)si - i \tag{9}$$
$$\dot{r}(t) = i \tag{10}$$

This set satisfies the constraint $s + i + r = 1$ and it is subject to initial conditions:

$$i(0) = i_0; \quad s(0) = s_0 = 1 - i_0; \quad r(0) = 0. \tag{11}$$

Equations (8)-(10) contain the single dimensionless parameter R_0, also commonly denoted as the reproduction number and assumed to express the expected number of secondary infections generated by an infected individual. We point out that this interpretation is actually incomplete, since it does not specify the interval of time over which such infections will occur. The following simple calculation shows the difficulty inherent to such an interpretation.

Ignore for a moment the dependence of R_0 on r, and take s constant. Then, equations (8)-(9) give

$$i \approx i_0 \exp\left[(R_0 - 1)t\right] \tag{12}$$

which is the familiar exponential rise in infections at the onset of the epidemic (if $R_0 > 1$). The cumulative total at time t is

$$\int_0^t i\, dt \approx \frac{i_0}{(R_0 - 1)} \left[\exp\left[(R_0 - 1)t\right] - 1\right] \tag{13}$$

If we were to take R_0 to be the average number of new infections caused by an average infected person, namely for the relation $R_0 = (\int_0^t i\, dt)/i_0$ to hold, we must specify the time interval, t_{R_0}, given by equation

$$t_{R_0} = \frac{\ln[1 + R_0(R_0 - 1)]}{(R_0 - 1)} \tag{14}$$

Clearly, t_{R_0} is not constant and depends on R_0 itself. For example, for $R_0 = 2$, 4 (or 250) we find $t_2 = 1.09$, $t_4 = 0.85$ (or $t_{250} = 0.044$) corresponding to about 15 days, 12 days (or 15 hours), respectively, under the present normalization. While more refined estimates are possible, given that the infection curve ceases to be exponential after some time, it is clear that interpreting R_0 as the ratio of secondary infections to initial infections is not well-posed. For this reason, we will elect to consider R_0 as simply a dimensionless parameter that measures in a monotonic fashion the intensity of contagiousness and the strength of the infection rate.

Qualitative as it might be, this observation is significant in relation to super-spreader events or events that follow different infection kinetics. Typically, super-spreader events occur over a time of the order of a few hours, which in the present dimensionless notation, expressed with a characteristic time of 14 days, is very small (e.g., roughly 0.015 for an event of 5 hrs duration). Using the standard SIR model, it follows that for a significant infection to occur during these events, the corresponding R_0 must be very large during that time interval. We will explore whether this is indeed the case by obtaining a quantitative estimate for such events. It is also important to anticipate that while the rate expressions in (3)-(5) depend linearly on i (through the product is), this will not necessarily be representative of the kinetics in enclosed environments, where air circulation and the dynamics of infection may cause longer-range interactions, giving rise to behavior not captured by (1). This is a key point of this paper and is further discussed below. A signal of a qualitatively different behavior is that parameter R_0 of the conventional SIR model becomes time-dependent during such events.

2.1 Modeling Infection in Enclosed Environments for Short Duration Events

Consider, now, an enclosed-environment event (e.g. a super-spreader event), starting at time t^* and lasting over the interval T_{ss}, where $\epsilon = T_{ss}/T_r \ll 1$. For example, for $T_{ss} = 5$ hr and a recovery time scale characteristic of COVID-19 ($T_r = 14$ days $= 336$ hr) we have $\epsilon \approx 0.015$. Take, next, the conventional SIR model (based on the one-to-one interaction) and assume that it also applies during the event. For this, we must allow R_0 to be time-dependent (which will be shown below to be necessary since the one-to-one infection kinetics are not valid

in an enclosed environment). By rescaling time around t^*, and defining $\tau = (t - t^*)/\epsilon$, equations (8)-(10) read

$$\frac{ds}{d\tau} = -\epsilon R_0(t^* + \epsilon\tau, r^*)si \tag{15}$$

$$\frac{di}{d\tau} = \epsilon R_0(t^* + \epsilon\tau, r^*)si - \epsilon i \tag{16}$$

$$\frac{dr}{d\tau} = \epsilon i \tag{17}$$

For such short-duration events, the limit $\epsilon \to 1$ applies. This implies that the recovered fraction remains practically constant, $r \approx r^*$, thus

$$s + i \approx s_+ + i_+ \approx s_- + i_- = c^* = 1 - r^*. \tag{18}$$

where subscript $+$ denotes states after the conclusion of the event and subscript $-$ denotes states before the event. The sum c^* of susceptible and infected individuals is constant at the onset, during the event, and at the conclusion of the event. Inserting (18) in equation (16) then gives

$$\frac{di(\tau)}{d\tau} = \epsilon R_0(t^* + \epsilon\tau; r^*)(c^* - i)i \tag{19}$$

which can be integrated to yield

$$\frac{i}{(c^* - i)} = \frac{i_-}{s_-} \exp\left[c^*\epsilon \int_0^\tau R_0(t^* + \epsilon\tau; r^*)d\tau\right]. \tag{20}$$

At the conclusion of the event ($t - t^* = \epsilon$, namely $\tau = 1$), infected and susceptible fractions are given by

$$i_+ = \frac{i_- c^* \exp[c^* b_1]}{s_- + i_- \exp[c^* b_1]} \tag{21}$$

and

$$s_+ = \frac{s_- c^*}{s_- + i_- \exp[c^* b_1]}. \tag{22}$$

respectively. Here, we also defined a quantity that represents the cumulative action of R_0 during the event,

$$b_1 \equiv \epsilon \int_0^1 R_0(t^* + \epsilon\tau; r^*)d\tau. \tag{23}$$

Clearly, for non-trivial changes in infection to occur during such an event, R_0 must be significantly large (order of ϵ^{-1}), suggesting a delta-function-like behavior. As expected, $s_+ < s_- < 1$, $i_+ > i_-$, while the maximum of i_+ is c^*, reached when $s_+ = 0$, namely when all susceptible individuals are infected at the conclusion of the event. Conversely, when $c^* b_1 \ll 1$, the event is not of the super-spreader kind, i.e., $i_+ \approx i_-$ and $s_+ \approx s_-$. We note that (21) and (22) are valid regardless of the type of evolution of the epidemic prior to the event as they only depend on the values i_- and s_-. We also remark that the above results apply to all short duration events, whether or not they correspond to enclosed environments. The effect of the latter is addressed in the next section.

2.2 Infection Kinetics in Enclosed Environments and R_0

We now turn to the question of what are actually the true kinetics in enclosed environment events (whether or not of the super-spreader type) where airborne transmission is suspected [4, 5], and what are the corresponding values of R_0 (and b_1) over short duration events. To make progress we will ignore for the moment the SIR model and use instead the *Wells-Riley* framework for transmission risk [5, 9–12]. In such models, the increase in the infected fraction is given by the following

$$i_+ - i_- = p_t s_- \tag{24}$$

where the *transition probability* p_t is defined as

$$p_t = 1 - \exp\left(-\frac{D}{D_i}\right). \tag{25}$$

Here, D denotes the cumulative pathogen intake (e.g., the number of SARS-CoV-2 RNA copies for COVID-19) for an individual at the event and D_i the dose that leads to transmission in roughly 63% of the cases.

Comparing (24) and (25) with (21) shows that the SIR model formalism cannot capture these kinetics. Indeed, if we were to force an agreement between the two it would require a time-varying R_0 and a dependence on the process parameters, likely including the initial conditions as well, which is contrary to the expected constancy of R_0 in the SIR framework. However, this mismatch is indeed expected given the different kinetic rates assumed in the two models. One way to reconcile the two would be to view the enclosed environment short-duration event using a similar effective chemical reaction formalism as in (1) but with a different stoichiometry, namely

$$S + \frac{1}{m} I \mapsto \frac{1}{m} I + I \tag{26}$$

where m is the number of susceptible individuals that can be infected at the same time by an infected individual, and further take $m \to \infty$. In that limit, the reaction rate will not depend on species I, thus we can write instead of (19) the following

$$\frac{di}{d\tau} = \epsilon R_{0,\infty} s = \epsilon R_{0,\infty}(c^* - i), \tag{27}$$

where the new parameter $R_{0,\infty}$ is the prefactor in rate expression corresponding to (26) at $m \to \infty$ (the rate being only proportional to s) and the subscript ∞ is used to indicate the large m limit. Implicit to (27) is also the previous assumption that the event is of a small duration, thus allowing us to neglect any recovery of infected individuals.

Integrating (27) and evaluating at the end of the event then yields

$$i_+ - i_- = (c^* - i_-)\left[1 - \exp(-b_\infty)\right] = s_-\left[1 - \exp(-b_\infty)\right] \tag{28}$$

where

$$b_\infty \equiv \epsilon R_{0,\infty}. \tag{29}$$

It follows that equation (28) is identical to the model in equations (24)-(25), subject to the identification

$$b_\infty = \frac{D}{D_i}. \tag{30}$$

We conclude that the enclosed environment kinetics can be captured using the one-to-m infection rate formalism of (26) in the large m limit. We can make further progress by using the simplified *well-mixed room* model [13], and express the normalized virus dose for a susceptible individual at the event as

$$\frac{D}{D_i} = \frac{C_{ss} Q T_{ss}}{D_i}, \tag{31}$$

Here, Q is the typical volumetric respiration rate ($\mathrm{m^3 hr^{-1}}$) and C_{ss} is the average airborne virus concentration (virus RNA copies $\mathrm{m^{-3}}$). Assuming steady state conditions, limited settling due to gravity and no virus decay, the latter can be approximated by

$$C_{ss} = \frac{\rho i_-}{h V_{ac}} E_i, \tag{32}$$

where h (m) is the height of the room, V_{ac} ($\mathrm{hr^{-1}}$) is the ventilation air change rate, and E_i (virus RNA copies $\mathrm{hr^{-1}}$) is the average virus emission rate by an infectious individual. Combining (30) with (31)-(32), we finally find

$$b_\infty = \frac{\rho i_- Q T_{ss}}{h V_{ac}} \frac{E_i}{D_i} \tag{33}$$

and

$$R_{0,\infty} = \frac{b_\infty}{\epsilon} = \frac{\rho i_- Q T_r}{h V_{ac}} \frac{E_i}{D_i}. \tag{34}$$

Note that filtering effects due to the presence of face coverings (i.e., masks) can be included in the expressions above to lower the dosage and emission rates estimates. We also note that, in addition to the initial fraction i_-, the RHS of (34) is proportional to two dimensionless groups, one that is process and operation-dependent $\frac{\rho Q}{h V_{ac}}$ and another that depends on physiological and biological conditions $\frac{T_r E_i}{D_i}$.

Equation (34) is an expression for the prefactor to the infection rate dependence for conditions of enclosed environment and a short duration event. Therefore, it is the equivalent expression to (7) for the SIR model. However, the prefactor $R_{0,\infty}$ is proportional to the *initial* fraction of infected population, i_-, thus underscoring the different kinetics involved. It is the first such relation derived to our knowledge and complements its counterpart expression for the one-to-one kinetic rate expression in (7) . For completeness, we also note that for consistency in terminology we could use $R_{0,1}$ to denote the R_0 in the SIR model (which has the one-to-one stoichiometry of (1), thus $m = 1$) but have elected not to, in order to avoid confusion.

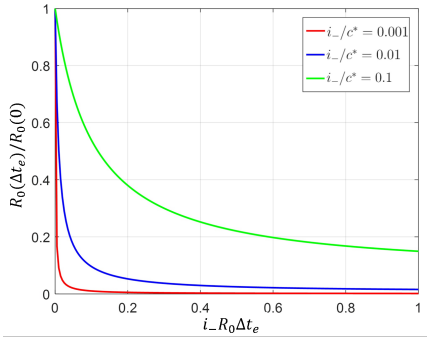

Figure 1. The effect of the duration of the event on the value of R_0, for three different values of $\frac{i_-}{c^*}$.

2.3 Super-Spreader Events

Consider, now, super-spreader events. To generate quantitative estimates for b_∞ and $R_{0,\infty}$, we assume the following conditions consistent with COVID-19 super-spreader events. Prior work suggests that infectious individuals can emit well over 100 quanta (infectious doses D_i) per hour when actively vocalizing [5, 12]. We assume a 50% duty cycle such that the average normalized emission rate is $E_i/D_i \approx 50$ hr^{-1}. We further assume: limited spatial distancing ($\rho \approx 0.25$ m^{-2}); an average room height ($h = 2.5$ m); low ventilation rates ($V_{ac} = 2$ hr^{-1}); a moderate respiration rate ($Q = 0.36$ m^{3}hr^{-1}); and no facial coverings. For $T_{ss} = 5$ hr and $T_r = 336$ hr, this yields $b_\infty = 4.5 i_-$ and $R_{0,\infty} = 302 i_-$ (e.g., $R_{0,\infty} = 30.2$ for $i_- = 0.1$). If we interpret $R_{0,\infty}$ as the reproduction parameter for super-spreader events in enclosed environments, the above findings are consistent with the expectation that super-spreader events have large values of the reproduction parameter. For example, for $i_- = 0.1$ and $s_- = 0.9$, the final fraction of infected population is $i_+ = 0.45$, more than four times the initial over that very short period of time. The corresponding number for $i_- = 0.01$ is 0.043, again, more than a four-fold increase.

Next, we consider if and how one could apply the traditional SIR model for enclosed environment and short duration event conditions, even though its kinetics are different. To do this we combine (21), (24) and (25) to find

$$\exp[c^* b_1] = \frac{c^*}{i_-} \exp\left(\frac{D}{D_i}\right) - \frac{s_-}{i_-}. \tag{35}$$

Assuming b_1 now represents the cumulative action of R_0 up to time $\tau = (t - t^*)/\epsilon$ during the event, the above expression can be differentiated with respect to time to yield

$$R_0(t - t^*) = \frac{R_{0,\infty}}{\left(c^* - s_- \exp\left(-\frac{D}{D_i}\right)\right)} \tag{36}$$

Because D varies with the duration of the event, this expression is also time-varying, thus demonstrating that the SIR model is intrinsically unsuitable for describing the process. At the onset of the event, we have

$$R_0(0) = \frac{R_{0,\infty}}{i_-} = \frac{\rho Q}{h V_{ac}} \frac{T_r E_i}{D_i}, \tag{37}$$

which for the parameters above corresponds to a large value of about 302. As the event continues, however, R_0 decreases monotonically. In a more compact notation, we can then rewrite (36) as

$$\frac{R_0(\Delta t_e)}{R_0(0)} = \frac{i_-}{(c^* - s_- \exp(-i_- R_0(0) \Delta t_e))} \tag{38}$$

where we have used the dimensionless event duration $\Delta t_e = \frac{T_{ss}}{T_r} = \epsilon$. Figure 1 shows that the value of R_0 decreases monotonically, asymptotically stabilizing to

$$\frac{R_0(\infty)}{R_0(0)} = \frac{i_-}{c^*} \tag{39}$$

The fact that R_0 is not a constant, but varies with the duration of the event, is a demonstration that the infection kinetics during the event are not accurately captured with a linear dependence of the infection rate on i, as assumed in the SIR-type model, but rather require the different interpretation along the lines suggested in (27).

One concludes that use of the standard SIR model under super-spreader events will lead in general to a value of R_0 that depends on the event duration, suggesting that the enclosed-room kinetics may not be properly captured. The appropriate approach for such cases would be to keep the dependence on I fixed at the initial infection conditions, in which case one obtains a revised and more appropriate constant value, $R_{0,\infty}$.

3 Concluding Remarks

In this paper, we focused on obtaining an understanding of the reproduction parameter R_0. We showed that the traditional assumption, inherent to the SIR model, that infection occurs by one-to-one interaction between an infected and a susceptible individual, fails to capture events where the interaction is by one to many (m) individuals (e.g., in enclosed environments). We provided an approach that models such different interactions by proposing a different reaction-like model stoichiometry, described in (26). This approach was used to model super-spreader events ($m \gg 1$) and can also be generalized to a model that captures finite m kinetics. We will present the results of such an analysis in a forthcoming publication. Despite its lack of applicability, the traditional SIR model can still be used to model a super-spreader event, if one accounts for the fact that R_0 will be time-dependent. Note that this time dependence is not physical, but rather it enables a fit to the predictions of a model with the correct physicochemical infection characteristics. We showed that the impact of an enclosed environment event is significant such that the initial value of the reproduction number R_0 is substantial ($O(100)$). Using a well-mixed room model and a different rate dependence on the infected fraction we demonstrated that such behavior is indeed expected for physicochemical, operational, and physiological conditions representative of known indoor COVID-19 super-spreader events. The impact of super-spreader events to an epidemic is substantial at its earlier stages, acting as a catalyst for nucleating new infections with potentially measurable effects on the approach to herd immunity. The effect of other kinetics, corresponding to finite values of m is currently under further study.

Acknowledgements. ML acknowledges support from the USC Viterbi School of Engineering.

Authorship statement. The authors hereby confirm that they are the sole liable persons responsible for the authorship of this work, and that all material that has been herein included as part of the present paper is either the property (and authorship) of the authors, or has the permission of the owners to be included here.

References

[1] H. Ramaswamy, A. A. Oberai, and Y. C. Yortsos. A comprehensive spatial-temporal infection model. *Chemical Engineering Science*, vol. 233, pp. 116347, 2021.
[2] R. M. Anderson and R. M. May. Population biology of infectious diseases: Part i. *Nature*, vol. 280, n. 5721, pp. 361–367, 1979.
[3] H. W. Hethcote. The mathematics of infectious diseases. *SIAM review*, vol. 42, n. 4, pp. 599–653, 2000.
[4] J. Lu, J. Gu, K. Li, C. Xu, W. Su, Z. Lai, D. Zhou, C. Yu, B. Xu, and Z. Yang. COVID-19 outbreak associated with air conditioning in restaurant, Guangzhou, China, 2020. *Emerging infectious diseases*, vol. 26, n. 7, pp. 1628, 2020.
[5] S. L. Miller, W. W. Nazaroff, J. L. Jimenez, A. Boerstra, G. Buonanno, S. J. Dancer, J. Kurnitski, L. C. Marr, L. Morawska, and C. Noakes. Transmission of sars-cov-2 by inhalation of respiratory aerosol in the skagit valley chorale superspreading event. *Indoor air*, vol. 31, n. 2, pp. 314–323, 2021.
[6] J. O. Lloyd-Smith, S. J. Schreiber, P. E. Kopp, and W. M. Getz. Superspreading and the effect of individual variation on disease emergence. *Nature*, vol. 438, n. 7066, pp. 355–359, 2005.
[7] A. James, J. W. Pitchford, and M. J. Plank. An event-based model of superspreading in epidemics. *Proceedings of the Royal Society B: Biological Sciences*, vol. 274, n. 1610, pp. 741–747, 2007.
[8] W. O. Kermack and A. G. McKendrick. A contribution to the mathematical theory of epidemics. *Proceedings of the royal society of london. Series A, Containing papers of a mathematical and physical character*, vol. 115, n. 772, pp. 700–721, 1927.
[9] E. Riley, G. Murphy, and R. Riley. Airborne spread of measles in a suburban elementary school. *American journal of epidemiology*, vol. 107, n. 5, pp. 421–432, 1978.
[10] C. J. Noakes and P. A. Sleigh. Mathematical models for assessing the role of airflow on the risk of airborne infection in hospital wards. *Journal of the Royal Society Interface*, vol. 6, n. suppl_6, pp. S791–S800, 2009.
[11] G. N. Sze To and C. Y. H. Chao. Review and comparison between the Wells–Riley and dose-response approaches to risk assessment of infectious respiratory diseases. *Indoor air*, vol. 20, n. 1, pp. 2–16, 2010.
[12] G. Buonanno, L. Stabile, and L. Morawska. Estimation of airborne viral emission: Quanta emission rate of sars-cov-2 for infection risk assessment. *Environment international*, vol. 141, pp. 105794, 2020.
[13] W. W. Nazaroff. Indoor bioaerosol dynamics. *Indoor Air*, vol. 26, n. 1, pp. 61–78, 2016.